

Published in final edited form as:

Neurosci Lett. 2012 June 27; 520(1): 38–42. doi:10.1016/j.neulet.2012.05.026.

Expression of the P/Q (Cav2.1) calcium channel in nodose sensory neurons and arterial baroreceptors

Milos Tatalovic¹, Patricia A. Glazebrook¹, and Diana L. Kunze^{1,2,*}

¹Rammelkamp Center for Education and Research, Case Western Reserve University, 2500, MetroHealth Drive, Cleveland OH 44109

²MetroHealth Campus and Department of Neurosciences, Case Western Reserve University, 2500, MetroHealth Drive, Cleveland OH 44109

Abstract

The predominant calcium current in nodose sensory neurons, including the subpopulation of baroreceptor neurons, is the N-type channel, Cav2.2. It is also the primary calcium channel responsible for transmitter release at their presynaptic terminals in the nucleus of the solitary tract in the brainstem. The P/Q channel, Cav2.1, the other major calcium channel responsible for transmitter release at mammalian synapses, represents only 15–20% of total calcium current in the general population of sensory neurons and makes a minor contribution to transmitter release at the presynaptic terminal. In the present study we identified a subpopulation of the largest nodose neurons (capacitance > 50pF) in which, surprisingly, Cav2.1 represents over 50% of the total calcium current, differing from the remainder of the population. Consistent with these electrophysiological data, anti-Cav2.1 antibody labeling was more membrane delimited in a subgroup of the large neurons in slices of nodose ganglia. Data reported in other synapses in the central nervous system assign different roles in synaptic information transfer to the P/Q-type versus N-type calcium channels. The study raises the possibility that the P/Q channel which has been associated with high fidelity transmission at other central synapses serves a similar function in this group of large myelinated sensory afferents, including arterial baroreceptors where a high frequency regular discharge pattern signals the pressure pulse. This contrasts to the irregular lower frequency discharge of the unmyelinated fibers that make up the majority of the sensory population and that utilize the N-type channel in synaptic transmission.

Keywords

Cav2.1; P/Q-type calcium channel; nodose; baroreceptor

© 2012 Elsevier Ireland Ltd. All rights reserved.

Rammelkamp Center R326, MetroHealth Medical Center, 2500 MetroHealth Drive, Cleveland, OH 44109-1998., Tel.: +216 778 8967; fax: 216 778 2090, dxk35@case.edu.

Publisher's Disclaimer: This is a PDF file of an unedited manuscript that has been accepted for publication. As a service to our customers we are providing this early version of the manuscript. The manuscript will undergo copyediting, typesetting, and review of the resulting proof before it is published in its final citable form. Please note that during the production process errors may be discovered which could affect the content, and all legal disclaimers that apply to the journal pertain.

Introduction

Nodose sensory neurons express several types of calcium channels including L-type (Cav1.2 and Cav1.3), N-type (Cav2.2), T-type (Cav3.2) and P/Q-type (Cav2.1) calcium channels. The N-type channels (ω -conotoxin GVIA-sensitive) represent approximately 60% of the peak calcium current in the general population of nodose neurons with P/Q-type channels (ω -agatoxin IVA-sensitive) contributing 16% (1). In that study the authors correlated the calcium currents recorded in the soma with those driving transmitter release at the synaptic terminal. They found block of N-type calcium channels reduced the evoked synaptic current by 57% while P/Q-type block reduced release by 12%. Thus, the current profile was similar at the soma and the presynaptic terminal.

In immunohistochemical studies of the distribution of calcium channels in nodose ganglion neurons, a subset of the largest neurons more strongly labeled at the membrane with an antibody against the P/Q-type calcium channel. In this study, we asked whether the P/Q-type channel provided the major calcium current present in the soma of these neurons, differing from the general population. We found that in a small subgroup of large nodose neurons including soma of aortic arch arterial baroreceptors, the P/Q-type current represents approximately 50–60% of the total calcium current in contrast to the lower percentage of 16% reported from the nodose population as a whole (1).

As we are particularly interested in the arterial baroreceptors, we also asked whether Cav2.1 distribution extended to the sensory terminals of the myelinated axons which represent the low threshold, tonically active baroreceptors. We found that the anti-Cav2.1 strongly labeled the sensory terminal, including the plate-like structures characteristic of the terminal region of large myelinated fibers.

Methods

All animal use protocols were reviewed and approved for ethical practice by the Institutional Animal Care and Use Committee of Case Western Reserve University and was in accord with NIH guidelines.

Nodose culture preparation

Rats (5–6 weeks) were sacrificed by decapitation under isoflurane anesthesia and the nodose ganglia were extracted, cut into thirds and placed in cold nodose complete media (NCM; composed of DMEM F-12 (Gibco) supplemented with 5% fetal bovine serum (FBS; Cellgro) and 1% penicillin-streptomycin-neomycin antibiotic mixture (PSN; Gibco). The ganglia were transferred to an enzyme solution containing 1.0 mg/ml collagenase type II (Worthington) in Earle's balanced salt solution (Gibco) for 70–80 minutes at 37°C. The enzyme solution was removed and replaced with NCM containing 1.5 mg/ml bovine albumin (Sigma) and the ganglia were dissociated by trituration with fire-polished pipettes. Cells were plated on poly-D-lysine-coated glass coverslips.

Electrophysiology

Electrophysiological experiments were performed on adult nodose neurons cells at room temperature, 3–12 hours after plating. Using a whole-cell patch configuration under voltage-clamp conditions, data were obtained with an Axopatch-1C patch clamp, digitized and analyzed using pCLAMP (Axon Instruments). The extracellular solution for voltage-clamp experiments contained (mM): 139 tetraethylammonium chloride, 2 BaCl₂, 5.4 KCl, 10 Glucose, 10 HEPES, and 5 4-Aminopyridine, pH 7.4. Electrodes (2–4 M Ω) prepared for voltage-clamp contained (mM): 124 CsCl, 10 HEPES, 1 CaCl₂, 11 EGTA, 2 MgCl₂, pH was adjusted to 7.2. Stock solution of ω -agatoxin IVA (Sigma) was made in distilled water to concentration of 1.0 mM and stored at –20°C until further diluted in bath solution (10nM to 1 μ M) on the day of the experiment. While a full concentration response curve was not performed, a concentration of 10nM was less effective than 100nM while a concentration of 1 μ M produced no additional block of calcium current. Therefore, the experiments reported here utilized a concentration of 100nM. In a subset of experiments we blocked the Cav2.2 (N-type) channel with ω -conotoxin GVIA at a concentration of 1 μ M (1). The voltage clamp protocol consisted of a –100 mV pre-pulse (duration of 30 ms) from a holding potential of –80 mV, followed by a 400 ms pulse to a step voltage between –70 and +20 mV in 10 mV increments. Peak current elicited at each voltage step was measured to construct the current-voltage relationship. Amplitude of the current was adjusted to cell capacitance and expressed as pA/pF. Statistics are present as mean \pm se.

Immunohistochemistry

Sprague-Dawley rats, weighing approximately 100g, were anesthetized by isoflurane inhalation and decapitated. The nodose ganglia were removed, embedded in OCT compound (Tissue-Tek) and sectioned by cryostat. Sections were mounted on Fisherbrand Superfrost/Plus slides, left in fixative overnight and rinsed in phosphate buffered saline (PBS). After fixation, the tissue sections were incubated with blocking solution containing 10% normal donkey serum, 1% bovine serum albumin, and 0.3% Triton-X-100 (TX-100) in PBS for 30 minutes. Primary antibody, anti-Cav2.1 (rabbit polyclonal, Alomone ACC-001 Lot #9) was diluted in PBS containing 1% BSA with 0.3% TX-100 and sections were incubated with primary antibody overnight at 4°C. Following brief rinses in PBS, the sections were incubated with the fluorescent labeled secondary antibody, diluted in blocking solution, for 90 minutes at room temperature. Tissue sections were rinsed again in PBS and mounted with Vectashield (Vector Laboratories). A Nikon E600 microscope equipped with a Spot RT Camera or the Leica SP2 spectral confocal microscope was used for imaging the sections. In a subset of tissue slices the Cav2.1 antibody was preabsorbed in a 1:10 dilution with the peptide supplied. Labeling was absent on these tissue sections which were processed at the same concentration as the untreated antibody on adjacent sections of ganglion.

Isolation and immunohistochemistry of the aortic arch terminals and aortic depressor nerve

Sprague-Dawley rats at 5–6 weeks of age were anesthetized by isoflurane inhalation and subsequently decapitated. A section of the proximal aortic depressor nerve (ADN) was removed and quick frozen in OCT (Tissue-Tek) in isopentane on dry ice. The nerve was

cryosectioned in 6 μm cross-sections and collected on SuperPlus Slides (Fisher Scientific). The slides were blocked in PBS containing 10% normal donkey serum (NDS), 0.3% TX-100, 1% BSA (Jackson ImmunoResearch) for 30 minutes. The primary antibodies, a cocktail of rabbit anti-Cav2.1 (1:200) and mouse anti-myelin basic protein (Chemicon MAB381, lot# 23010518) (1:300) and were incubated on the slides 3 hr at room temperature. After rinsing in PBS the secondary cocktail, containing donkey anti-rabbit Red X and donkey anti-Mouse FITC (Jackson ImmunoResearch), was applied for 90 minutes. The sections were imaged using the Leica Microsystem SP2 Confocal microscope. In another set of animals, the region of the aortic arch containing the innervation by the aortic ADN was isolated, cut lengthwise along the inferior surface and laid flat with the inner vessel wall facing up. The muscle was peeled away, leaving only the adventitia containing the nerve terminals. The tissue was prepared for immunohistochemistry as previously described (3). The antibodies used in this study included the previously mentioned as well as anti-Na/K ATPase $\alpha 3$ (Santa Cruz Biological SC-16052 lot# F2206). Imaging was performed using the Leica Microsystem SP2 Confocal microscope. Sequential serial stacks were collected for reconstruction of the nerve terminals using Autoquant software (MediaCybernetics, Silver Spring, MD).

Labeling arterial baroreceptors—The aortic depressor nerve, carrying the aortic arch baroreceptor fibers, was labeled with the fluorescent anterograde tracer DiA (4-(4-dihexadecylaminostyryl)-N-methylpyridinium iodine, Molecular Probes) (4). The animal allowed to recover 5–7 days before nodose ganglia were isolated for culture or immunohistochemistry.

Results

Cav2.1 is ubiquitously expressed in nodose sensory neurons

As expected based on previous electrophysiological studies, anti-Cav2.1 staining was present in most neurons of the nodose ganglion in internal compartments and near or in the membrane (Fig.1A). Thus, the Cav2.1 is present in the soma of visceral sensory neurons conveying sensory information from the cardiovascular, respiratory and gastrointestinal systems. Staining levels varied among neurons within the population, however labeling in/near the membrane was most striking in the larger diameter neurons where it was highly concentrated at/near the membrane as shown at higher magnification in figure 1B.

Anti-Cav2.1 is present in baroreceptor axons and in the peripheral sensory terminals of large myelinated arterial baroreceptors

We addressed the localization of Cav2.1 in one set of visceral sensory receptors, the arterial baroreceptors. In cross-sections of the aortic depressor nerve which carries arterial baroreceptor afferents, the anti-Cav2.1 labeling was present in both myelinated fibers identified with anti-myelin basic protein and in surrounding, presumably, unmyelinated fibers (Fig.1C).

Myelinated arterial baroreceptors axons extend form branching plate-like sensory terminals (5, 6). An example is shown in figure 1D which includes the myelinated axon and its

terminal region, identified by co-labeling with an anti-Na/KATPase- α 3 subunit antibody (6) and an anti-myelin basic protein antibody. This demonstrates the plate-like structure of the terminal of a myelinated fiber. Expression of Cav2.1 is shown in figure 1E where a terminal region like that in figure 1D co-labels with anti-Cav2.1 antibody and anti-Na/KATPase- α 3 subunit antibody. Similar results were obtained in the two other terminals of the same type from two different preparations. Anti-Cav2.1 labeling of unmyelinated terminals was not readily apparent either because it was not present or because of the paucity of expression in these thin fibers.

ω -agatoxin IVA-sensitive current supplies the majority of calcium current in a subset of large nodose neurons

Previous studies demonstrated that ω -agatoxin IVA, a Cav2.1 channel blocker, reduced total calcium current by about 16% in the general population of sensory neurons which consists primarily (85%) of C-type neurons with unmyelinated axons (1). In the present study we evaluated the calcium current using barium as the ion carrying species. Initially we biased recordings toward the larger neurons but extended the study to include smaller cells for comparison to a previous study (1). The aortic depressor nerve was labeled with DiA in 2 animals to identify baroreceptor soma. A voltage-clamp protocol (Methods) was used to elicit total calcium current (Fig. 2A). ω -agatoxin IVA (ω -AgaTx, 100 nM) was then added to the perfusate to identify the Cav2.1 component. The percentage of block by the toxin fell into two distinct groups, greater than 50% or less than 30%.

The composite current-voltage relationship for seven of the neurons with large ω -AgaTx responses (inhibition > 50% peak current) is shown in figure 2B (lower panel). The peak current measured at -10 mV was reduced significantly from -67 ± 19 pA/pF to -28 ± 7 pA/pF ($p < 0.03$, two sample, paired t-test). Two of these seven neurons were DiA-labeled from the aortic depressor nerve. We also show the composite current voltage relationship of six of neurons where peak calcium current was reduced <30% from -45.0 ± 5 pA/pF to -36 ± 10 pA/pF ($p < 0.05$, upper panel). One of the latter was DiA labeled as a baroreceptor neuron.

The % inhibition for individual neurons is plotted against the cell capacitance (Fig. 2C). The inhibition for the 10 neurons with >50% inhibition (encircled) was $67 \pm 3\%$ (range 52–88%) and for the 27 neurons with inhibition <30% was $15 \pm 1\%$ (range 7–29%). As can be seen in this figure, not all large capacitance neurons express the high level of ω -AgaTx current.

In a subset of neurons, we compared the percent block of the total peak current by the N-type (Cav2.2) blocker ω -conotoxin-GVIA (ω CTx) with that of the P/Q-type channel block by ω -AgaTx. For those neurons with a small Cav2.1 current the percent inhibition by ω -AgaTx, was 14% with a ω CTx block of 63% ($n=7$), consistent with previous studies. For those cells with a large agatoxin current, the block by ω -AgaTx was 70% and by ω CTx, 21% ($n=3$).

Discussion

Cav2.1 is present in nodose neurons as indicated by the presence of anti-Cav2.1 immunoreactivity and the ω -agatoxin IVA-sensitive currents recorded in the soma. This study identified a subset of these sensory neurons that expresses Cav2.1 as the predominant calcium current (> 50% of total peak calcium current) in contrast to the majority of cells in which N-type current prevails and where P/Q-type current accounts for only 15–20% of the total calcium current (1 and present study). Within the entire population of nodose neurons, approximately 15% of have myelinated axons and are subclassified as A β or A δ based on conduction velocity measurements (8). The remaining 85% of nodose neurons fall into the C-type class with unmyelinated axons. The neurons expressing majority P/Q currents are large diameter cells with capacitance in the range of 50–95 pF, likely to include the A β cells and the largest of the A δ cells. The population of the neurons with capacitance in this range may have been previously overlooked in sampling cultured neurons as it represents only a small proportion (4%) of the total number of cells (7). The study raises two questions concerning the role of the P/Q-type channel at the peripheral and central terminals.

Role of P/Q-type channels at the peripheral sensory terminal

While we have shown that P/Q immunoreactivity is present in the sensory terminals of large myelinated baroreceptors, its role at this site is unknown. The activity of the terminal region cannot be recorded directly. Instead, extracellular recordings of the baroreceptor discharge are obtained from the axons some distance from the terminal. Using that preparation, a previous report indicates that P/Q channel inhibitor ω -agatoxin IVA does not affect the discharge of myelinated fibers in an isolated perfused aortic arch preparation (1). Access of the toxin to the terminal from the internal perfusate may be problematic, but these authors also applied the toxin to the external adventitial surface. Thus, published data at present do not support a direct role for Cav2.1 in the transduction process.

Role of P/Q-type channels at the central presynaptic terminal

The study also raises the question of whether the P/Q-type current is primarily responsible for transmitter release at the central presynaptic terminal of this subgroup of neurons. Data presented from other synapses in the central nervous system implicate the P/Q channel in transmission at synapses that 1) conserve the fidelity of information transfer and 2) are not highly regulated by G-protein receptor mediated modulation of action potential duration and, therefore, transmitter release (9–13). This is of interest because the population of large myelinated arterial baroreceptor neurons responds to its stimulus, the arterial pressure pulse, with a clearly defined and highly reproducible, high frequency discharge which would be expected to be preserved across the synapse. In these A-type neurons the short duration action potentials measured at the soma are not readily modulated by either frequency or neuromodulators (7, 15). This contrasts with the discharge of C-type fibers that compose 85% of the population of visceral sensory afferents and that exhibit irregular lower frequency discharge patterns (14). They have broad action potentials that are modulated by frequency (7) and by a variety of neurotransmitters (15). In these C-type neurons, activation or inhibition of Cav2.1 by neuromodulators at the presynaptic terminal may serve to regulate

synaptic activity even though it is not the primary channel responsible for evoked transmitter release.

Conclusions

We have identified a distinct group of nodose sensory neurons which expresses the P/Q-type calcium current as its major calcium current in contrast to the majority of nodose neurons for which the N-type current predominates. Just as the N-type channel is primarily responsible for transmitter release at the central terminal in the general population, we propose that the P/Q type channel will underlie transmitter release in the subpopulation identified in the present study consistent with the functional role of the large myelinated afferent fibers. The role of P/Q at the presynaptic terminal in the nucleus of the solitary tract can be tested when the central termination site of this small group of fibers is identified. Because of the likelihood that not all of the neurons with a large P/Q component are baroreceptors, it will be interesting to examine the relative calcium components of other high fidelity transmitting visceral afferents.

Acknowledgments

This work was supported by NIH HL090886 (DLK).

References

1. Mendelowitz D, Reynolds PJ, Andresen MC. Heterogeneous functional expression of calcium channels at sensory and synaptic regions in nodose neurons. *J Neurophysiol.* 1995; 73:872–875. [PubMed: 7760142]
2. Evans RM, Zamponi GW. Presynaptic Ca²⁺ channels--integration centers for neuronal signaling pathways. *Trends Neurosci.* 2006; 29:617–624. [PubMed: 16942804]
3. Doan T, Stephans K, Glazebrook PA, Ramirez A, Andresen MC, Kunze DL. Differential distribution and function of hyperpolarization-activated channels (I_H) in sensory neurons and mechanosensitive fibers. *J Neurosci.* 2004; 24:3335–3343. [PubMed: 15056713]
4. Mendelowitz D, Kunze DL. Characterization of calcium currents in aortic baroreceptor neurons. *J Neurophys.* 1992; 68:509–517.
5. Krauhs JM. Structure of rat aortic baroreceptors and their relationship to connective tissue. *J Neurocytol.* 1979; 8:401–414. [PubMed: 490188]
6. Wladyka CL, Feng B, Schild JH, Kunze DL. The KCNQ/M current modulates arterial baroreceptor function at the sensory terminal in rats. *J Physiol.* 2008; 586:795–802. [PubMed: 18048450]
7. Li BY, Glazebrook P, Kunze DL, Schild JH. KCa1.1 channel contributes to cell excitability in unmyelinated but not myelinated rat vagal afferents. *Am J Physiol Cell Physiol.* 2011; 300:C1393–1403. [PubMed: 21325638]
8. Li BY, Schild JH. Electrophysiological and pharmacological validation of vagal afferent fiber type of neurons enzymatically isolated from rat nodose ganglia. *J Neurosci Methods.* 2007; 164:75–85. [PubMed: 17512602]
9. Ishikawa T, Kaneko M, Shin H-S, Takahashi T. Presynaptic N-type and P/Q-type Ca²⁺ channels mediating synaptic transmission at the calyx of Held of mice. *J Physiol.* 2005; 568:199–209. [PubMed: 16037093]
10. Inchauspe CG, Forsythe ID, Uchitel OD. Changes in synaptic transmission properties due to the expression of N-type calcium channels at the calyx of Held synapse of mice lacking P/Q-type calcium channels. *J Physiol.* 2007; 584:835–851. 835. [PubMed: 17823210]
11. Colecraft HM, Brody DL, Yue DT. G-protein inhibition of N- and P/Q-type calcium channels: distinctive elementary mechanisms and their functional impact. *J Neurosci.* 2001; 21:1137–1147. [PubMed: 11160384]

12. Fedchyshyn MJ, Wang LY. Developmental transformation of the release modality at the calyx of Held synapse. *J Neurosci.* 2005; 25:4131–40. [PubMed: 15843616]
13. Li L, Bischofberger J, Jonas P. Differential gating and recruitment of P/Q-, N-, and R-type Ca²⁺ channels in hippocampal mossy fiber boutons. *J Neurosci.* 2007; 27:13420–13429. [PubMed: 18057200]
14. Thorén P, Saum WR, Brown AM. Characteristics of rat aortic baroreceptors with nonmedullated afferent nerve fibers. *Circ Res.* 1977; 40:231–237. [PubMed: 837469]
15. Higashi H, Ueda N, Nishi S, Gallagher JP, Shinnick-Gallagher P. Chemoreceptors for serotonin (5-HT), acetylcholine (ACh), bradykinin (BK), histamine (H) and gamma-aminobutyric acid (GABA) on rabbit visceral afferent neurons. *Brain Res Bull.* 1982; 8:23–32. [PubMed: 7055734]

Highlights

We evaluated the presence of P/Q type calcium channel in nodose sensory neurons

The P/Q-type channel supplies the major calcium current in subset of large neurons

This contrasts the majority of nodose cells where N-type channels predominate

We postulate a dominant P/Q channel preserves a high fidelity signal at the synapse

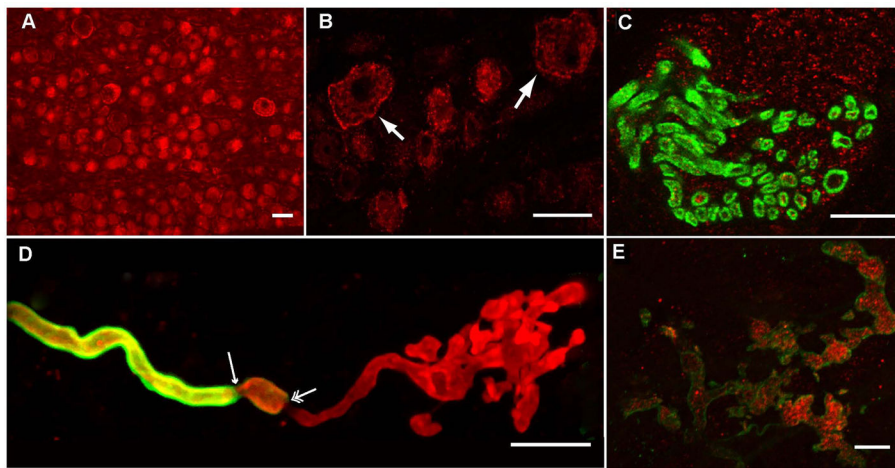


Figure 1. Cav2.1 is ubiquitously expressed in nodose sensory neurons

A) Anti-Cav2.1 staining (red) was broadly present in neurons in sections of nodose ganglion in this Spot camera image. Scale bar = 35 μm . **B)** Several larger cells in this higher magnification image show strong labeling at the membrane (arrows). Scale bar = 35 μm . **C)** Cav2.1 is present in the aortic depressor nerve which carries the aortic arch baroreceptor afferent axons. In this confocal image of a cryosection of the aortic depressor nerve, the anti-Cav2.1 labeling (red) was present inside myelinated fibers labeled with myelin basic protein (green). Presumed, labeled unmyelinated fibers are also present (red alone). Scale bar = 15 μm . **D)** An example of a myelinated arterial baroreceptor terminal constructed from a confocal stack of images illustrates the loss of preterminal myelin as the axon forms the plate like structure of sensory ending. The nerve terminal was labeled with anti-Na/KATPase $\alpha 3$ antibody (red) and the myelin with anti-MBP antibody (green). The myelin starts to thin on the nerve fiber (single arrow) then in a short distance the myelin ends totally (double arrow). The nerve fiber continues on and branches out to form convoluted plate-like structures that have anti-Na/KATPase- $\alpha 3$ immunolabeling. Scale bar = 25 μm . **E)** The plate-like structures of a myelinated terminal are labeled with anti-Cav2.1 antibody (red) in this series of sequential confocal images collected through terminal that has been labeled with anti-Na/KATPase- $\alpha 3$ subunit (green). Scale bar = 5 μm .

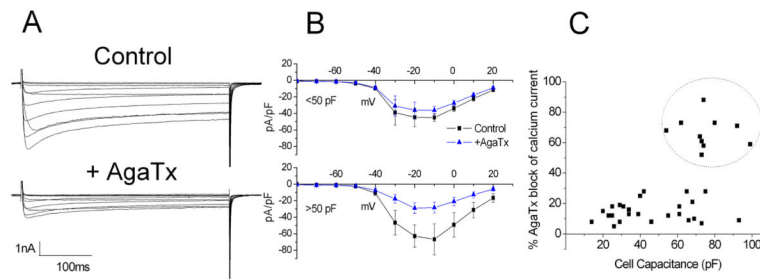


Figure 2. ω -agatoxin IVA-sensitive channels supply the majority of calcium current in a subset of large nodose neurons

A) Control currents are shown in the upper set of traces in response to a series of 400 ms depolarizing steps from -70 mV to $+20$ mV. Application of ω -agatoxin IVA (100 nM) reduced peak calcium current in this neuron approximately 65%. B) The composite current-voltage relationships for six cells with ω -agatoxin IVA block of $<30\%$ (upper) and seven neurons that responded with a block of over 50% of the current (lower). C) Plot of % inhibition of peak calcium current by ω -agatoxin IVA versus cell capacitance for individual neurons identifies a high capacitance subgroup for which over 50% of the calcium current is ω -agatoxin IVA-sensitive current (encircled).